World Scientific
www.worldscientific.com

One-step hydrothermal synthesis of NiS/MoS₂-rGO composites and their application as catalysts for hydrogen evolution reaction

Huaping Wu*, Ye Qiu*, Junma Zhang†, Guozhong Chai*, Congda Lu*,§,‖
and Aiping Liu*,†,‡,¶,‖

*Laboratory of E&M (Zhejiang University of Technology)
Ministry of Education & Zhejiang Province
Hangzhou 310014, P. R. China

†Center for Optoelectronics Materials and Devices
Zhejiang Sci-Tech University, Hangzhou 310018, P. R. China

‡State Key Laboratory of Nonlinear Mechanics, Institute of Mechanics
Chinese Academy of Sciences, Beijing 100190, P. R. China
§lcd@zjut.edu.cn
¶liuaiping1979@gmail.com

The composites of sulphide and reduced graphene oxide (NiS/MoS₂-rGO) were synthesized through a facile solvent-assisted hydrothermal method. The introduction of NiS was paramount not only in enhancing the conductivity of whole catalysts but also in modulating the layer structures of MoS₂ with additional active sites. Moreover, the NiS and rGO functioned together in controlling the morphology of as-prepared composites, resulting in uniformly distributed NiS/MoS₂ nanosheets perpendicular to rGO scaffold. This further contributed to the excellent hydrogen evolution performance of the composites with a small onset overpotential of 80 mV and Tafel slope as low as 65 mV/decade.

Keywords: NiS/MoS₂-rGO composites; hydrothermal method; hydrogen evolution reaction.

Hydrogen associated with its clean and sustainable property has been widely considered as one of the most suitable alternates to traditional nonrenewable and environment-polluted energy resources to meet the energy crisis. Among all of hydrogen preparation techniques, water electrolysis has aroused great attention due to the convenient and cost-effective preparation process.[1,2] Up to now, platinum and its composites are hailed as the state-of-the-art hydrogen evolution reaction (HER) catalysts in the acid media.[3–5] However, the high cost and low earth-abundance limit their further application[6–8] and finding an ideal candidate is therefore urgent.[9–11]

Recently, nano-sized MoS₂ with catalytic active sites stemming from edges of (002) crystal planes has been demonstrated as an efficient HER catalyst.[10,11] Tremendous efforts have been carried out to design nano-sized MoS₂, aiming at creating more active sites or improving the conductivity.[11,12] Toward this end, combining conductive metals,

such as Ni,[6] Pt,[1] Cu[4] and Co,[5] with layered MoS₂ has been regarded as an effective solution to improve HER activity by modifying the electronic structure of MoS₂ nanosheets. Especially, the effective combination of nickel ions with MoS₂ is preponderant when considering the lower production cost and easier synthesis process.[7,8] For example, Li and his co-workers successfully incorporated nickel ions into MoS₂ microspheres, resulting in responsible HER performance due to improved intrinsic conductivity.[7] Wu et al. proved that small amount of nickel ions could favor the creation of electrochemical active sites.[8] In addition, graphene or reduced graphene oxide (rGO), a typical two-dimensional material with unique electron mobility, large surface area, excellent mechanical and chemical stability, is widely used as templates to anchor nano-sized materials to adjust the morphology and conductivity of catalysts.[11] However, as far as we know, there is far less explored research related to the structural variety and electrocatalytic tunability of layered MoS₂ nanosheets when combined with nickel ions and graphene/rGO together.


‖Corresponding authors.

H. Wu et al.

In this work, we presented a facile one-step solvent-assisted hydrothermal method to synthesis NiS/MoS$_2$-rGO composites. GO was found to play key roles in controlling NiS/MoS$_2$-rGO morphology, resulting in uniformly distributed NiS/MoS$_2$ nanosheets perpendicular to the rGO scaffold. Moreover, the successful introduction of nickel ions not only effectively prevented layered MoS$_2$ nanosheets from aggregation, but also created more defect as active sites, which further favored the HER performance with a small overpotential of 80 mV and low Tafel slope of 65 mV/decade. This work provides a facile way to prepare NiS/MoS$_2$-rGO composites as HER catalysts and may open up a new horizon to synthesize similar composites.

GO was synthesized according to previous reported method.[12] For NiS/MoS$_2$-rGO preparation, typically, 0.5 mL of GO suspension (9 mg/mL), 0.1 g of Na$_2$MoO$_4$·2H$_2$O, 0.05 g of NiCl$_6$·6H$_2$O and 15 mL of mixed solvent (Glycol and H$_2$O with a volume ratio of 2:1) were stirred together. Then the obtained solution was sonicated for 1 h and transferred to a 25 mL Teflon-lined stainless steel autoclave and maintained at 220°C for 20 h, followed by naturally cooling down to room temperature. Then the obtained product was washed by ethanol for several times and dried overnight. The MoS$_2$-rGO and NiS/MoS$_2$ samples as references were synthesized through similar produces except NiCl$_6$·6H$_2$O and GO addition, respectively. In order to investigate the effect of hybrid composition on the structure and performance, different NiS/MoS$_2$-rGO hybrids were prepared by changing the mass ratios of precursors (NiCl$_6$·6H$_2$O/Na$_2$MoO$_4$·2H$_2$O) from 1:8 to 1:1.

Morphologies and microstructures of hybrids were recorded on a field emission scanning electron microscope (FESEM, Hitachi S4800) equipped with an energy-dispersive X-ray spectroscopy (EDS) and a transmission electron microscopy (TEM, Hitachi H-7650). Crystalline structures of hybrids were obtained on a X-ray diffractometer (Bruker AXS D8) using the Cu Ka radiation. X-ray photoelectron spectroscopy (XPS) was collected by a KRATOS AXIS ULTRA-DLD. All electrochemical measurements were conducted on a CHI 660D electrochemical work station (Shanghai Chenhua Instrument Co., China) in a three-electrode cell. A 3 mm-diameter glassy carbon electrode, saturated calomel electrode (SCE) and platinum wire were used as the working, reference and counter electrodes, respectively. For electrode preparation, 5 mg catalyst power and 60 μL Nafion solution (5 wt.%) were dispersed in 1 mL water-ethanol solution with volume ratio of (3:1) and sonicated for 0.5 h to form a homogeneous ink. Then 5 μL suspension was drop-casted on the working electrode (loading ca. 0.325 mg×cm^{-2}). Linear sweep voltammetry (LSV) measurement with a scan rate of 5 mV/s was conducted in a

0.5 M H$_2$SO$_4$. AC impendence measurements were carried out in the same configuration at an overpotential of 0.165 V (frequency range: 10^5–0.1 Hz with an AC voltage of 5 mV). All potentials were calibrated to reversible hydrogen electrode (RHE). All data were iR compensated.

Figure 1(a) shows X-ray diffraction (XRD) patterns of different catalysts. For MoS$_2$-rGO, the peaks located at 8.9°, 32.4° and 58.4° can be assigned to the (002), (100) and (110) crystal planes of hexagonal MoS$_2$ (JCPDS No. 37-1492).[6,13] Notice that the (002) crystal planes shift to 8.9°, indicating the enlarged layer distance during the hydrothermal process.[11] The NiS/MoS$_2$ exhibits four obvious peaks located at 30.0°, 34.5°, 45.7° and 53.4°, indicating NiS existence (JCPDS No. 02-1280).[14] However, the diffraction peak at 8.9° related to MoS$_2$ is weaker, suggesting NiS introduction can prevent MoS$_2$ nanosheets from aggregation.[15] Moreover, (002) crystal plane peak disappears for NiS/MoS$_2$-rGO (mass ratio of precursors is 1:2), which could be attributed to the fact that rGO further inhibits MoS$_2$ growth along the (002) crystal planes.[11] The EDS result (Fig. 1(b)) exhibits the atom ratio of Ni/Mo/S is about 1:1.4:3.8, further confirming
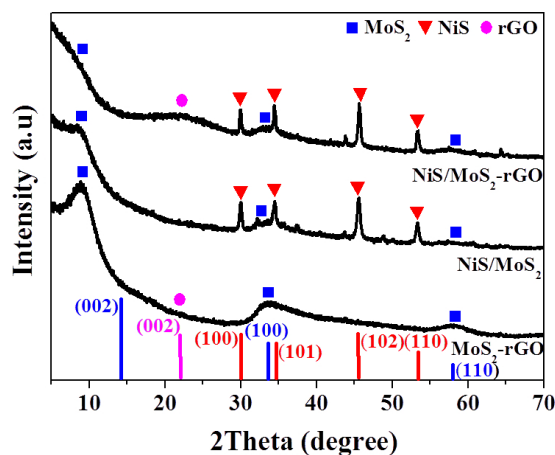
(a)
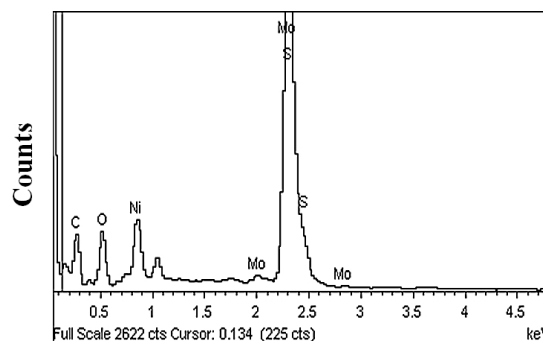
(b)

Fig. 1. (a) XRD patterns of MoS$_2$-rGO, NiS/MoS$_2$ and NiS/MoS$_2$-rGO composites, (b) EDS for NiS/MoS$_2$-rGO composites. The mass ratio of precursors is 1:2.
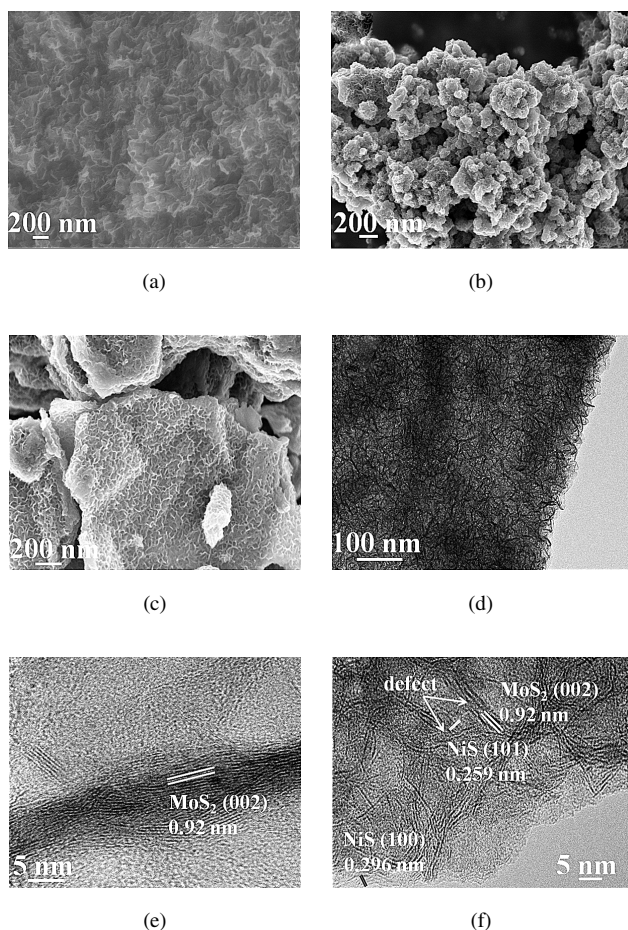
(a)

(b)

(c)

(d)

(e)

(f)

Fig. 2. SEM images of (a) MoS$_2$-rGO, (b) NiS/MoS$_2$ and (c) NiS/MoS$_2$-rGO. (d) TEM image of NiS/MoS$_2$-rGO and HRTEM images of (e) MoS$_2$-rGO and (f) NiS/MoS$_2$-rGO. The mass ratio of precursors is 1:2.

Table 1. Atomic percentage (at.%) compositions of different NiS/MoS$_2$-rGO hybrids prepared with different mass ratios of precursors.

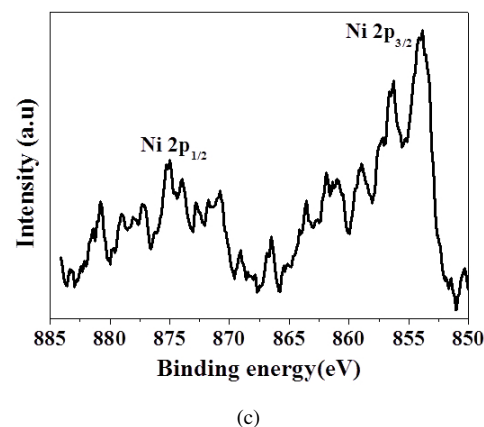| Sample	C	O	Ni	Mo	S
MoS$_2$-rGO	58.16	14.19	—	9.31	18.34
NiS/MoS$_2$	—	—	16.14	22.82	61.04
NiS/MoS$_2$-rGO (1:8)	54.03	13.85	2.79	8.93	20.40
NiS/MoS$_2$-rGO (1:4)	51.48	13.91	4.71	8.47	21.43
NiS/MoS$_2$-rGO (1:2)	49.77	14.83	5.67	8.04	21.69
NiS/MoS$_2$-rGO (1:1)	49.49	15.97	6.53	7.18	20.83

(a)

(b)

(c)
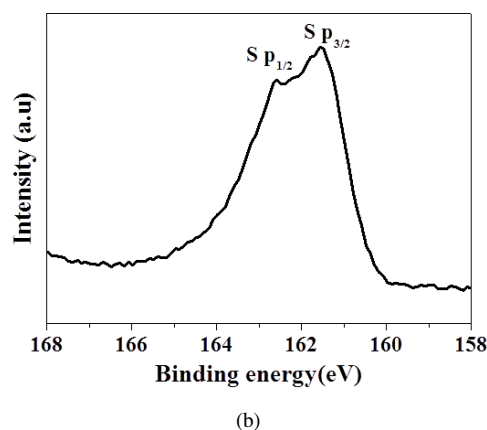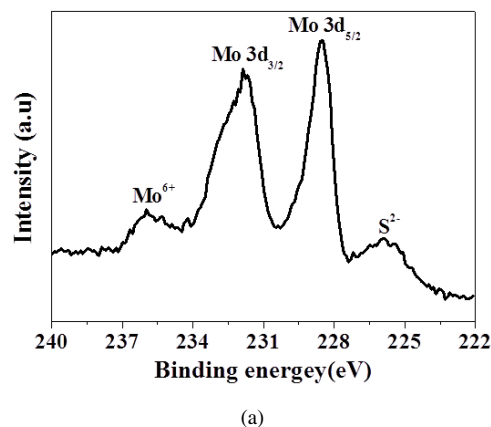
Fig. 3. XPS spectra of NiS/MoS$_2$-rGO composites: (a) Mo3d, (b) S2p and (c) Ni2p. The mass ratio of precursors is 1:2.

NiS/MoS$_2$-rGO formation, which is in good agreement with XRD results.

Figure 2(a) shows scanning electron microscope (SEM) image of MoS$_2$-rGO. The curved MoS$_2$ nanosheets tightly stack together and are tiled on rGO surface. The NiS/MoS$_2$ composites (Fig. 2(b)) are composed of various sized nanosheets with intertwined and aggregated together. When GO suspension is introduced in the reaction system, vertical nanosheets with 70 nm lengths are homogeneously distributed on rGO surface (Figs. 2(c) and 2(d)), indicating the fact that both NiS and GO play significant roles in controlling NiS/MoS$_2$-rGO morphologies. Noting that MoS$_2$ sheets in NiS/MoS$_2$-rGO have less layers (< 5, Fig. 2(f)) than those in MoS$_2$/rGO (Fig. 2(e)), suggesting the introduction of nickel ions could inhibit MoS$_2$ nanosheets from stacking along the *C*-axis,[15] which is in good agreement with XRD results (Fig. 1(a)). Moreover, three lattice fringes with interlayer distance of 0.259, 0.296 and 0.90 nm could be assigned to (101) and (100) crystal planes for NiS[16] and enlarged (002) crystal plane for MoS$_2$,[11,13] respectively. In addition, NiS addition introduces more additional defects, as indicated by

arrows in Fig. 2(f), which is helpful for HER performance improvement.[5,13]

The average compositions of different NiS/MoS$_2$-rGO hybrids prepared with different mass ratios of precursors were obtained by XPS measurements at six different areas on the sample surfaces, as shown in Table 1. The atom ratio of Ni/Mo/S is about 1:1.4:3.8, which is in good agreement with EDS result and confirms the NiS/MoS$_2$-rGO formation. XPS curves (Fig. 3) further reveal element chemical states in NiS/MoS$_2$-rGO composites. The peaks located at 228.5 and 231.9 eV (Fig. 3(a)) could be attributed to Mo3d$_{5/2}$ and Mo3d$_{3/2}$,[1,11] respectively. Two characteristic peaks at 161.6 and 162.7 eV (Fig. 3(b)) correspond to the S2p$_{3/2}$ and S2p$_{1/2}$, respectively.[4,7] The peaks located at 853.9 and 875.1 eV (Fig. 3(c)) indicate Ni^{2+} ions presence in the composites.[6–8,14]

The influence of introduced Ni on catalytic activity is also investigated. The NiS/MoS$_2$-rGO composites (mass ratio of precursors of 1:2) present a rather small onset overpotential of 80 mV (Fig. 4(a)), which is approximately 60 mV and 153 mV smaller than those of NiS/MoS$_2$ and NiS-rGO, respectively. Moreover, NiS/MoS$_2$-rGO composites reach current density

of 40 mA/cm^2 at the overpotential of 300 mV, which is two times larger than that of reported Ni$_x$S$_y$-MoS$_2$ composites.[6] It is usually believed that the Tafel slope represents intrinsic properties of HER performance.[1,13] The Tafel slopes for NiS/MoS$_2$, MoS$_2$-rGO and NiS/MoS$_2$-rGO are 131, 80 and 65 mV/decade (Fig. 4(b)), respectively, indicating the HER mechanism for NiS/MoS$_2$-rGO follows the Volmer–Heyrovsky process with electrochemical desorption step as the rate-limiting step.[13] Such excellent HER activities of NiS/MoS$_2$-rGO could be reasoned as follows: (i) nickel ions introduction not only improves intrinsic conductivity of catalyst,[7] favors more active sites creation,[8] but also inhibits MoS$_2$ nanosheets from stacking;[15] (ii) NiS/MoS$_2$-rGO morphology could be effectively adjusted by the addition of GO and nickel precursors, resulting in homogeneously vertical MoS$_2$ nanosheets anchored on rGO surface, decreasing electron transfer resistance between adjacent layers;[11] (iii) rGO improves the conductivity of whole catalysts, promoting charge transfer process. However, excess nickel ions introduction might affect the loading amount of MoS$_2$ nanosheets by forming more NiS, decreasing the active sites for proton absorption and degrading HER performance, as shown in Fig. 5.
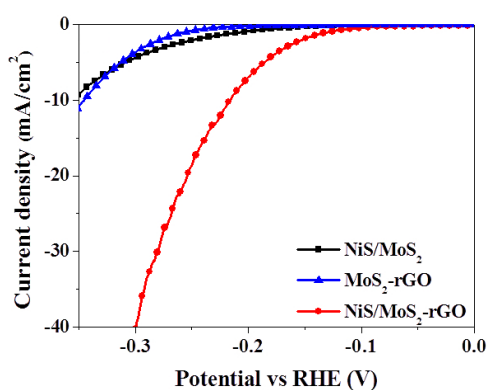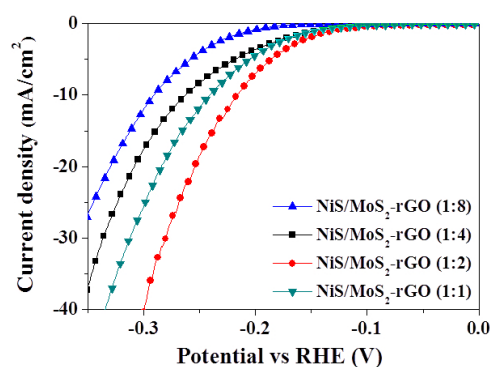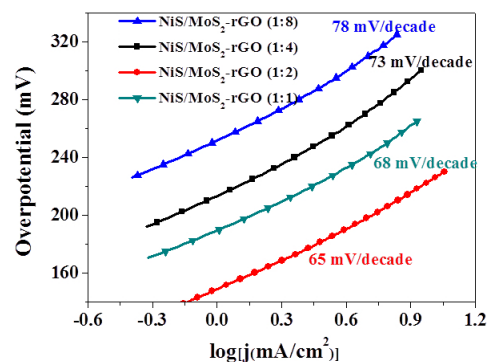

(a)
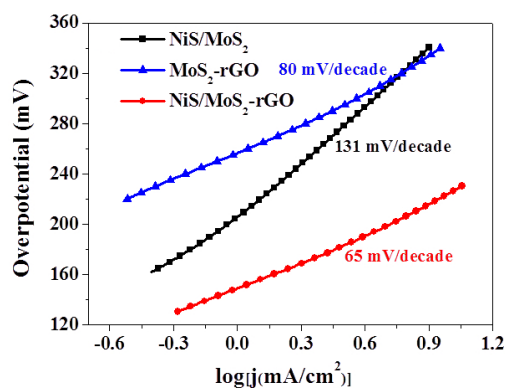
(b)

Fig. 4. (a) Polarization curves and (b) corresponding Tafel plots for MoS$_2$-rGO, NiS/MoS$_2$ and NiS/MoS$_2$-rGO composites.

(a)

(b)

Fig. 5. (a) Polarization curves and (b) corresponding Tafel plots for different NiS/MoS$_2$-rGO composites prepared with different mass ratios of precursors.

In summary, a facile one-step hydrothermal method has been developed to synthesize NiS/MoS$_2$-rGO composites. The GO and nickel precursors play critical roles not only in controlling composite morphology but also in improving HER performance by increasing conductivity and creating more active sites. The NiS/MoS$_2$-rGO composites with optimized composition ratio show a small onset overpotential of 80 mV and small Tafel slope as low as 65 mV/decade, indicating their potential as efficient catalysts for HER.

Acknowledgment

References

1. J. Deng *et al.*, *Energy Environ. Sci.* **8**, 1594 (2015).
2. H. Y. Jin *et al.*, *J. Am. Chem. Soc.* **137**, 2688 (2015).
3. X. Long *et al.*, *J. Am. Chem. Soc.* **137**, 11900 (2015).
4. D. Merki *et al.*, *Chem. Sci.* **3**, 2515 (2012).
5. F. Li *et al.*, *J. Power Sources* **292**, 15 (2015).
6. W. Cui *et al.*, *Electrochim. Acta* **137**, 504 (2014).
7. X. J. Lv *et al.*, *RSC Adv.* **3**, 21231 (2013).
8. D. Z. Wang *et al.*, *RSC Adv.* **6**, 16656 (2016).
9. B. Hinnemann *et al.*, *J. Am. Chem. Soc.* **127**, 5308 (2005).
10. T. F. Jaramillo *et al.*, *Science* **317**, 100 (2007).
11. X. L. Zheng *et al.*, *Chem. Mater.* **26**, 2344 (2014).
12. D. C. Marcano *et al.*, *ACS Nano* **4**, 4806 (2010).
13. J. F. Xie *et al.*, *J. Am. Chem. Soc.* **135**, 17881 (2013).
14. H. G. S. F. Kong and Y. Wang, *J. Mater. Chem. A* **2**, 15152 (2014).
15. J. W. Miao *et al.*, *Sci. Adv.* **1**, 1 (2015).
16. L. Tian *et al.*, *Cryst. Growth Des.* **9**, 352 (2009).